Relativistic bands in the discrete spectrum of created particles in an oscillating cavity

Danilo T. Alves,[1,*] Edney R. Granhen,[2,†] João Paulo da S. Alves,[3,‡] and Williams A. Lima[4,§]
[1]*Faculdade de Física, Universidade Federal do Pará, 66075-110 Belém, Pará, Brazil*
[2]*Instituto de Ciências Exatas, Faculdade de Física, Universidade Federal do Sul e Sudeste do Pará, 68505-080 Marabá, PA, Brazil*
[3]*Instituto Federal do Pará, 66093-020 Belém, PA, Brazil*
[4]*Observatório Nacional, 20921-400 Rio de Janeiro, RJ, Brazil*

(Received 16 September 2020; accepted 3 November 2020; published 2 December 2020)

We investigate the dynamical Casimir effect for a one-dimensional resonant cavity, with one oscillating mirror. Specifically, we study the discrete spectrum of created particles in a region of frequencies above the oscillation frequency ω_0 of the mirror. We focus our investigation on an oscillation time equal to $2L_0/c$, where L_0 is the initial and final length of the cavity, and c is the speed of light. For this oscillation duration, a field mode, after being perturbed by the moving mirror, never meets this mirror in motion again, which allows us to exclude this effect of reinteraction on the particle creation process. Then, we describe the creation of particles with energies above $\hbar\omega_0$, due only to the relativistic aspect of the mirror's velocity (and these particles form what we call relativistic bands). Thus, we analyze the formation of these relativistic bands in a discrete spectrum of created particles.

DOI: 10.1103/PhysRevD.102.125012

I. INTRODUCTION

Moore, in his pioneering paper on the dynamical Casimir effect (DCE) [1], pointed out that photons could be created by the excitation of the quantum vacuum by a moving mirror (the DCE was also investigated in other pioneering articles [2–5] and excellent reviews can be found in the literature [6–9]). On the other hand, he remarked that the photon creation predicted by him was too negligible to be detected experimentally [1]. One of the problems of particle creation via DCE is that, under laboratory conditions, the maximum velocity that an oscillating mirror can achieve is very small in comparison to the speed of light [10]. To circumvent this problem, Dodonov and Klimov investigated the possibility of the observation of the DCE considering a gradual accumulation of photons in a resonant cavity, so that a significant and measurable effect could be obtained [10]. Several other proposals have been made, focusing on the observation of particle creation from vacuum by experiments based on the mechanical oscillation of mirrors [11–16], but the observation remains a challenge [9].

From a more general point of view, particle creation from vacuum occurs when a quantized field is submitted to a time-dependent boundary condition. Therefore, a moving mirror exciting the vacuum is just a particular case. Yablonovitch [17] and Lozovik *et al.* [18] proposed alternative ways to excite the quantum vacuum, by means of time-dependent boundary conditions imposed on a material medium. Moreover, a motionless mirror whose internal properties rapidly vary in time can simulate a moving mirror. Several experimental proposals emerged in this context [19–26]. One of them led Wilson *et al.* to observe experimentally particle creation from vacuum [24], getting a maximum effective velocity $v \approx 0.1c$. Other experiments have also been done [25,27,28], with one of them getting a maximum effective velocity $v \approx 0.31c$ [28].

In the present paper, we investigate aspects of the problem by combining a resonant oscillating cavity with a relativistic maximum velocity of its moving mirror. Specifically, we study the discrete spectrum of created particles in the context of a real massless scalar field in $(1+1)$D, inside a resonant cavity with one relativistic moving mirror, oscillating with a frequency ω_0. Moreover, we impose the Dirichlet boundary condition to the field on the positions of the mirrors. We focus our investigation on the discrete spectrum of created particles in a region of frequencies above ω_0 (particles with energies above $\hbar\omega_0$), but considering an oscillation time $T = 2L_0/c$, where L_0 is the initial and final length of the cavity. Since for this oscillation duration a field mode, after being perturbed by the moving mirror, never meets this mirror in motion again, we exclude, in the creation of particles with frequencies above ω_0, the effect of the reinteraction of a perturbed field

*danilo@ufpa.br
†granhen@unifesspa.edu.br
‡joao.alves@ifpa.edu.br
§williamslima@on.br

mode with the mirror in a state of motion. Then, we isolate the effect of the maximum speed of the mirror in creating particles with frequencies above ω_0. The particles created with energies above $\hbar\omega_0$, due only to the relativistic aspect of the mirror's velocity, discarding the reinteraction effects, form what we call relativistic bands [29] (in contrast, a nonrelativistic band occurs, for instance, when a single nonrelativistic mirror, oscillating with a frequency ω_0, produces a spectrum of particles with energies lower than $\hbar\omega_0$ [30]). In this way, we describe, in a discrete spectrum of created particles, particle creation with frequencies above ω_0 caused only by the relativistic aspect of the mirror's motion (or the formation of relativistic bands). In the literature, works have investigated the formation of these relativistic bands, but in the context of continuous spectra for single mirrors (see Refs. [22,29,31]).

The paper is organized as follows. In Sec. II, we present the model to be investigated and write exact general formulas for the spectrum and total number of created particles in a dynamical cavity. In Sec. III, we make a brief check of the consistency of the exact formulas written in the previous section, comparing some of our results with analytical approximations found in the literature [10]. In Sec. IV, we calculate the spectrum of created particles for an oscillation time $T = 2L_0/c$, and discuss the appearance of relativistic bands. In Sec. V, we investigate the connection and consistency between the relativistic band in the discrete spectrum (found in the previous section) and the relativistic band in a continuous spectrum for a relativistic oscillating single mirror found in the literature [31]. In Sec. VI, we present a summary of our results and final comments.

II. EXACT FORMULAS FOR PARTICLE CREATION IN A CAVITY

Let us start by considering the massless scalar field in a two-dimensional spacetime satisfying the wave equation (we assume throughout this paper $\hbar = c = 1$)

$$(\partial_t^2 - \partial_x^2)\phi(t,x) = 0, \tag{1}$$

with the time-dependent boundary conditions

$$\phi(t,0) = \phi[t, L(t)] = 0, \tag{2}$$

where $L(t)$ is an arbitrary prescribed law for the moving boundary with $L(t<0) = L(t>T) = L_0$, where L_0 is the length of the cavity in the static situation, and T is the time at which the boundary returns to its initial position L_0 (see Fig. 1).

Considering the procedure adopted by Moore [1], and Fulling and Davies [3], the field in the cavity can be obtained by exploiting the conformal invariance of the wave equation (1). The field solution, in the Heisenberg representation $\phi(t,x)$, is given by

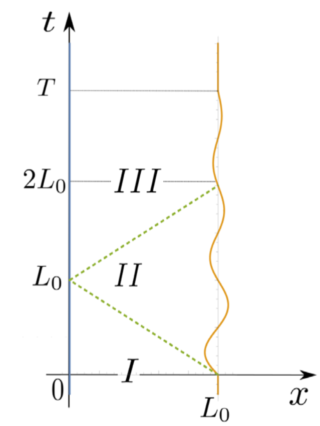

FIG. 1. Trajectories of the mirrors (solid lines). The static mirror is represented by the vertical solid (blue line) at $x = 0$. The moving mirror, oscillating around $x = L_0$, with $L(t<0) = L(t>T) = L_0$, is represented by the orange solid line. The dashed (green) lines are null lines separating region I from II, and region II from III.

$$\phi(t,x) = \sum_{n=1}^{\infty}[\hat{b}_n\phi_n(t,x) + \text{H.c.}], \tag{3}$$

where the field modes $\phi_n(t,x)$ are given by

$$\phi_n(t,x) = \frac{i}{\sqrt{4n\pi}}[e^{-in\pi R(v)} - e^{-in\pi R(u)}], \tag{4}$$

with $u = t - x$, $v = t + x$, and R satisfying Moore's functional equation:

$$R[t + L(t)] - R[t - L(t)] = 2. \tag{5}$$

For $t < 0$ (cavity in the static situation), $R(z) = z/L_0$ and the field $\phi(t,x)$ can be written in terms of the complete set of function $\phi_n^{(0)}(t,x)$ as [32]

$$\phi(t,x) = \sum_{n=1}^{\infty}[\hat{b}_n\phi_n^{(0)}(t,x) + \text{H.c.}], \tag{6}$$

where the field modes $\phi_n^{(0)}(t,x)$ are given by the relation

$$\phi_n^{(0)}(t,x) = \frac{i}{\sqrt{4n\pi}}[e^{-in\pi v/L_0} - e^{-in\pi u/L_0}], \tag{7}$$

with $[b_m, b_n^\dagger] = \delta_{mn}$. Similarly to Eq. (6), for $t > T$, when both boundaries are at rest again, the field solution $\phi(t,x)$ can be expanded as

$$\phi(t,x) = \sum_{n=1}^{\infty}[\hat{a}_n\phi_n^{(0)}(t,x) + \text{H.c.}]. \tag{8}$$

The new set of physical operators $(\hat{a}, \hat{a}^\dagger)$ is related to the old set $(\hat{b}, \hat{b}^\dagger)$ via the Bogoliubov transformation as

$$\hat{a}_m = \sum_{n=1}^{\infty}\{\hat{b}_n\alpha_{mn} + \hat{b}_n^{\dagger}\beta_{mn}^{*}\}, \tag{9}$$

with the Bogoliubov coefficients given by [33,34]

$$\alpha_{mn}(t) = \frac{1}{2}\sqrt{\frac{m}{n}}\int_{t/L_0-1}^{t/L_0+1} dx e^{-i\pi[nR(L_0x)-mx]},$$
$$\beta_{mn}(t) = -\frac{1}{2}\sqrt{\frac{m}{n}}\int_{t/L_0-1}^{t/L_0+1} dx e^{-i\pi[nR(L_0x)+mx]}, \tag{10}$$

where $R(z)$ is the solution of the Moore equation (5). The unitarity condition for the Bogoliubov transformation is written as $\sum_{n=1}^{\infty}[|\alpha_{mn}(t)|^2 - |\beta_{mn}(t)|^2] = 1$. The number $\mathcal{N}_n(t)$ of created particles in the cavity, in a certain mode n is given by

$$\mathcal{N}_n(t) = \sum_{m=1}^{\infty}|\beta_{nm}(t)|^2, \tag{11}$$

with $\beta_{nm}(t)$ given by Eq. (10). The total number $\mathcal{N}(t)$ of created particles in the cavity is given by

$$\mathcal{N}(t) = \sum_{n=1}^{\infty}\mathcal{N}_n(t). \tag{12}$$

Now, let us examine the cavity in the nonstatic situation ($t > 0$). According to Cole and Schieve [35], the field modes in Eq. (4) are formed by left- and right-propagating parts. As causality requires, the field in region I ($v \leq L_0$) (see Fig. 1) is not affected by the boundary motion, so that, in this sense, this region is considered as a “static zone.” In region II ($v > L_0$ and $u \leq L_0$), the right-propagating parts of the field modes remain unaffected by the boundary motion, so that region II is also a static zone for these modes. On the other hand, the left-propagating parts in region II are, in general, affected by the boundary movement. In region III ($u > L_0$), both the left- and right-propagating parts are affected. In summary, the functions corresponding to the left- and right-propagating parts of the field modes are considered in the static zone if their argument z (z symbolizing v or u) is such that $z \leq L_0$. For a certain spacetime point $(\tilde{t},\tilde{x})$, the field operator $\phi(\tilde{t},\tilde{x})$ is known if its left- and right-propagating parts, taken over, respectively, the null lines $v = z_1$ and $u = z_2$ (where $z_1 = \tilde{t} + \tilde{x}$ and $z_2 = \tilde{t} - \tilde{x}$), are known; or, in other words, $\phi(\tilde{t},\tilde{x})$ is known if $R(v)|_{v=z_1}$ and $R(u)|_{u=z_2}$ are known. Cole and Schieve [35] proposed an elegant recursive method to obtain exactly the function R for a general law of motion of the boundary. The method consists in tracing back a sequence of null lines intersecting the worldline of the moving mirror at instants t_i, until, after a certain number $i = n$ of reflections, a null line traced back gets into the static zone, where the function R is known. Following their procedure, one can write the solution of the Moore equation as [35–37]

$$R(z) = 2n(z) + \left[z - 2\sum_{i=1}^{n(z)}L(t_i)\right]/L_0, \tag{13}$$

where n is the number of reflections off the moving boundary, necessary to connect the null line $t + x = z$ (or $t - x = z$) to a null line in the static zone. Using Eq. (13) in Eqs. (11) and (12), we write the exact value for the number of created particles in the rth mode ($\mathcal{N}_{exa}^{(r)}$) and the total number of created particles $\mathcal{N}_{exa}$, respectively, by

$$\mathcal{N}_{exa}^{(r)}(t) = \sum_{s=1}^{\infty}\left|\frac{1}{2}\sqrt{\frac{r}{s}}\int_{t/L_0-1}^{t/L_0+1} dx e^{-i\pi[s\{2n(L_0x)+[L_0x-2\sum_{i=1}^{n(L_0x)}L(t_i)]/L_0\}+rx]}\right|^2, \tag{14}$$

$$\mathcal{N}_{exa}(t) = \sum_{r=1}^{\infty}\mathcal{N}_{exa}^{(r)}(t). \tag{15}$$

The formulas (14) and (15) are valid for an arbitrary prescribed law $L(t)$ for the moving boundary, provided that $L(t < 0) = L(t > T) = L_0$.

When one considers $L(t < 0) = L(t > T) = L_0$, $L(t)$ can present a discontinuity in the velocity of the mirror at $t = 0$ (and also at $t = T$), which can be responsible for a creation of an infinite number of particles [1,38]. In general, since the formulas (14) and (15) do not take into account such discontinuities, we can consider that they approximately describe particle creation for a law of motion $\tilde{L}(t)$ for which there is no discontinuity in its velocity, but that can be approximately described by the function $L(t)$. On the other hand, for $T = 2L_0$, the particles created by the discontinuity at $t = 0$ can be absorbed by the discontinuity at $t = T = 2L_0$ [39] (the main situation discussed in the present paper), so that particle creation in the cavity can be described exactly by the formulas (14) and (15).

In the next sections we will apply the formulas (14) and (15) to the following class of laws of motion for the moving mirror:

$$L(t) = \begin{cases} L_0, & t < 0, \\ L_0 + a\sin(2\pi t/l_0), & 0 \leq t \leq T, \\ L_0, & t > T \end{cases} \tag{16}$$

where $a > 0$ is the amplitude of oscillation, and l_0 needs to be chosen appropriately so that $L(t) = L_0$ for $t > T$.

Throughout the text, we consider $\omega_0 = 2\pi/l_0$ as the frequency of oscillation of the moving mirror.

III. COMPARISON WITH APPROXIMATE ANALYTICAL RESULTS

As a first application of our computations based on the exact formulas (14) and (15), we compare some of our results for the total number of created particles with those obtained by analytical approximations found in the literature [10]. Let us consider a particular resonant law of motion typically considered in the investigation of the DCE [10,32], given by Eq. (16) with $a = \varepsilon L_0$, $l_0 = L_0$, where $\varepsilon > 0$, and εL_0 is the amplitude of oscillation. Note that in this particular case the frequency $\omega_0 = 2\pi/L_0$ is twice the frequency of the first quantum mode, π/L_0, inside the static cavity of length L_0. This law of motion leads to resonant particle creation in the cavity. Dodonov and Klimov [10], considering this law of motion in the context of nonrelativistic velocities and low amplitudes, obtained perturbatively the approximate average total number of particles created, $\mathcal{N}_{app}$, as given by

$$\mathcal{N}_{app}(T) = \frac{1}{\pi^2}\left[\left(1 - \frac{\kappa^2}{2}\right)K^2(\kappa) - E(\kappa)K(\kappa)\right], \quad (17)$$

where $K(\kappa)$ and $E(\kappa)$ are the complete elliptic integrals of the first and second kind, respectively, and $\kappa = \sqrt{1 - e^{-4\varepsilon\pi T/L_0}}$. The authors also obtained the following formula for the number $\mathcal{N}^{(1)}_{app}$ of created particles in the first (fundamental) mode of the cavity:

$$\mathcal{N}^{(1)}_{app}(T) = \frac{2}{\pi^2}K(\kappa)E(\kappa) - \frac{1}{2}. \quad (18)$$

The results in Eqs. (17) and (18) were considered valid in the limit $\varepsilon \ll 1$ [10].

Let us compare the results for the total number of particles, using the formulas $\mathcal{N}_{exa}$ [Eq. (15)] and $\mathcal{N}_{app}$ [Eq. (17)]. We start this comparison by examining the case with $\varepsilon = 10^{-2}$, which implies a maximum velocity v of the mirror such that $v \approx 0.06$. In Fig. 2, corresponding to the case with $L_0 = 1$ ($\omega_0 = 2\pi$), one can see an agreement between $\mathcal{N}_{app}$ (circles) and $\mathcal{N}_{exa}$ (crosses). In addition, both results are in agreement with numerical ones found by Ruser [40] (other numerical approaches to solve DCE problems have also been developed [41–45]). We also verified agreement between $\mathcal{N}_{exa}$ [Eq. (15)] and $\mathcal{N}_{app}$ [Eq. (17)] for $s < -2$ in $\varepsilon = 10^s$.

Now, let us investigate the case with $\varepsilon = 10^{-1}$, which means a maximum velocity $v \approx 0.6$. In Fig. 3, one can see a certain disagreement between $\mathcal{N}_{exa}$ [Eq. (15)] and $\mathcal{N}_{app}$ [Eq. (17)], with $\mathcal{N}_{exa} > \mathcal{N}_{app}$ and $\mathcal{N}_{exa} - \mathcal{N}_{app}$ growing in time. It is worth mentioning that a similar disagreement (for $\epsilon = 10^{-1}$) was also observed in the literature [40],

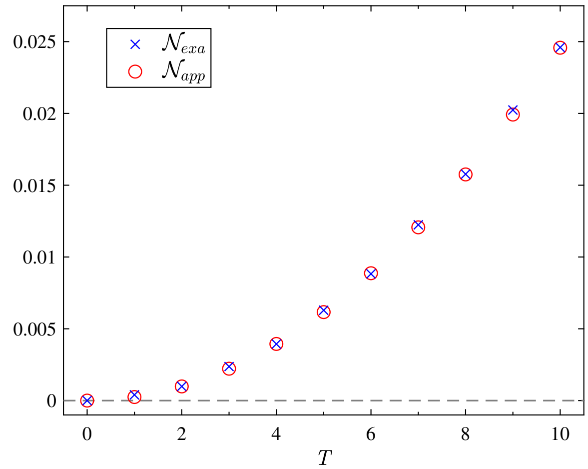

FIG. 2. Comparison between the number of particles (vertical axis) versus T (horizontal axis), via the approximate formula $\mathcal{N}_{app}$ (circles) and exact formula $\mathcal{N}_{exa}$ (crosses), for the law of motion given in Eq. (16), with $\varepsilon = 10^{-2}$ and $L_0 = 1$ ($\omega_0 = 2\pi$). The dashed line serves as a reference for the zero value of the number of particles.

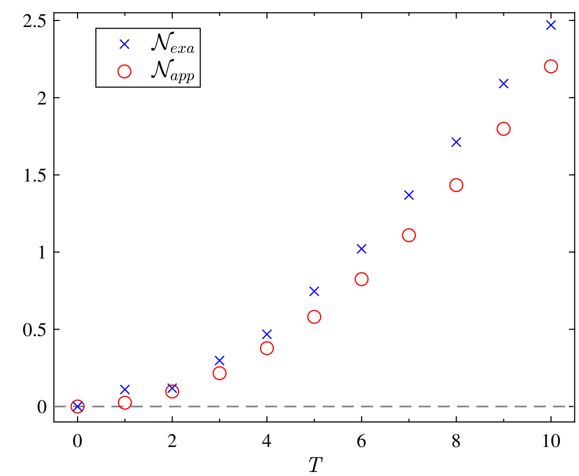

FIG. 3. Comparison between the number of particles (vertical axis) versus T (horizontal axis), via the approximate formula $\mathcal{N}_{app}$ (circles) and exact formula $\mathcal{N}_{exa}$ (crosses), for the law of motion given in Eq. (16), with $\varepsilon = 10^{-1}$ and $L_0 = 1$ ($\omega_0 = 2\pi$). The dashed line serves as a reference for the zero value of the number of particles.

when values calculated via numerical methods were compared to values from $\mathcal{N}_{app}$ [Eq. (17)]. This indicates that the disagreement found in Fig. 3 reveals not a failure in predictions based on $\mathcal{N}_{exa}$ [Eq. (15)], but a limit of validity for $\mathcal{N}_{app}$ [Eq. (17)] (namely, $\mathcal{N}_{app}$ is more valid for $s \leq -2$ in $\varepsilon = 10^s$).

IV. SPECTRUM OF CREATED PARTICLES

In a cavity with length L_0, with one of the mirrors in motion (for instance, the right one), the field modes, after being perturbed by the right oscillating mirror, are reflected by the left (static) mirror and go back to the right mirror again. If the field modes return to the right mirror and find that it is still in motion, the perturbed field modes undergo a new perturbation (reinteraction). On the other hand, if the perturbed field modes find the right mirror at rest, they are simply reflected, going in the opposite direction but with no new perturbation added to them. When reinteractions are allowed in an oscillating cavity (which happens when $T > 2L_0$), even with nonrelativistic velocities, particles can be produced with frequencies higher than the oscillation frequency [10,31,46]. For instance, for the law of motion in Eq. (16), with $l_0 = L_0$, $a = 10^{-8}L_0$ (which means $v = 2\pi \times 10^{-8}$) and $T > 2L_0$, particles can be created with frequencies $(2n+1)\pi/L_0$ $(n = 0, 1, 2...)$ and, for $n > 0$, with frequencies higher than $\omega_0 = 2\pi/L_0$ [10,46]. Then, the results in the literature [10,46] show that particle creation via DCE in the resonant cavity described by Eq. (16), with $T > 2L_0$, can be characterized by a discrete spectrum, the possibility of several reinteractions of the field modes with the moving mirror, and particles produced with frequencies higher than the oscillation frequency even with a nonrelativistic moving mirror.

In the present section we will focus on oscillatory motions obeying Eq. (16), with $l_0 = L_0$ and $T = 2L_0$ (see Fig. 4). This enables us to exclude the effect of the reinteraction of a perturbed field mode with the mirror in a state of motion, so that we can isolate only the role of the maximum speed of the mirror in creating particles with frequency above ω_0 (relativistic band). In this way, the relativistic band can be assigned exclusively to the relativistic aspect of the velocity of the mirror (as occurs for a relativistic single mirror [31]). This motion law is interesting because all field modes perturbed by the moving (right) mirror, after being reflected on the static (left) mirror at $x = 0$, go back to the right, but find the right mirror at rest. This is illustrated by the dashed lines in Fig. 4, which represent null lines related to the field modes perturbed by the right mirror in motion. In this manner, for the law of motion in Eq. (16) with $T = 2L_0$, the values of $\mathcal{N}^{(r)}_{exa}$ and $\mathcal{N}_{exa}$ exclude the effect of a new interaction of the perturbed field modes with the right mirror in the state of motion.

Considering the law of motion in Eq. (16), with $T = 2L_0$, $a = \varepsilon L_0$, $l_0 = L_0$, $\varepsilon = 10^{-2}$ $(v \approx 0.06)$, and using the exact formula (11), we obtain that there is no effective creation of particles with frequency above the oscillation frequency of the cavity $(2\pi/L_0)$, with the particle creation restricted to the fundamental mode $n = 1$ (π/L_0) (see Fig. 5), which has half of the oscillating frequency ω_0. This is in agreement with the approximate results found in the literature [10]. The expected number of particles $\mathcal{N}^{(1)}_{exa}$ obtained by us [via Eq. (14)] is in agreement with that obtained via the approximate formula $\mathcal{N}^{(1)}_{app}$ [Eq. (18)]: $\mathcal{N}^{(1)}_{exa} \approx \mathcal{N}^{(1)}_{app} \approx 0.001$.

Now, considering $\varepsilon = 10^{-1}$ $(v \approx 0.6)$ in Eq. (16) (with $T = 2L_0$ and $l_0 = L_0$), the exact method used here [Eq. (14)] also predicts, beyond creation in the fundamental mode $n = 1$ (π/L_0), particle creation in an additional band (frequencies larger than $\omega_0 = 2\pi/L_0$). For instance, in

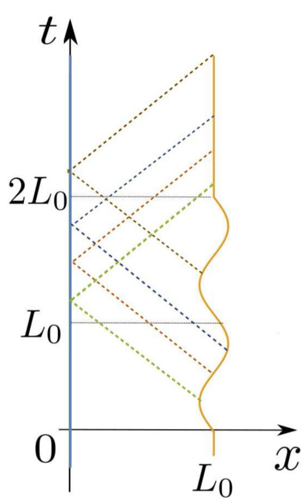

FIG. 4. Trajectories of the mirrors (solid lines). The static mirror is represented by the vertical solid (blue line) at $x = 0$. The trajectory of the moving mirror, according to Eq. (16) (with $l_0 = L_0$ and $T = 2L_0$), is given by the orange line. The dashed lines represent some null lines related to the field modes perturbed by the moving mirror. Note that, after being reflected by the left static mirror, all field modes, which were perturbed by the right mirror in motion, find the right mirror again already at rest.

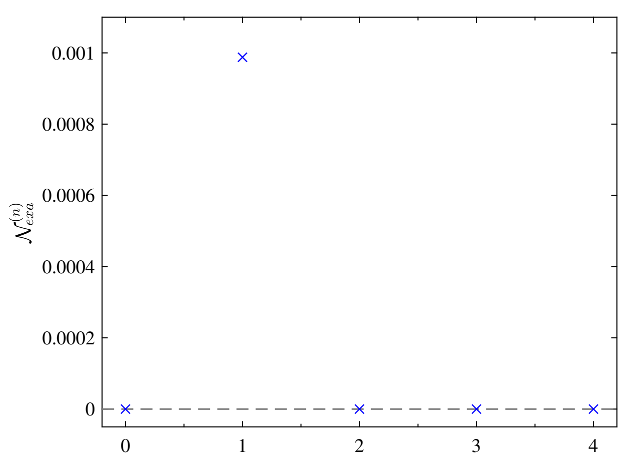

FIG. 5. The number of created particles $\mathcal{N}^{(n)}_{exa}$ (vertical axis) versus $n = \omega L_0/\pi$ (horizontal axis), for the law of motion given in Eq. (16), with $T = 2L_0$, $a = \varepsilon L_0$, $L_0 = l_0 = 1$ and $\varepsilon = 10^{-2}$ (maximum velocity $v \approx 0.06$). The dashed line serves as a reference for the value $\mathcal{N}^{(n)}_{exa} = 0$. Note that $n = 1$ represents half of the oscillation frequency, and $n = 2$ indicates the oscillation frequency ω_0. One can see no creation of particles with frequencies larger than $\omega_0 = 2\pi$ $(n = 2)$.

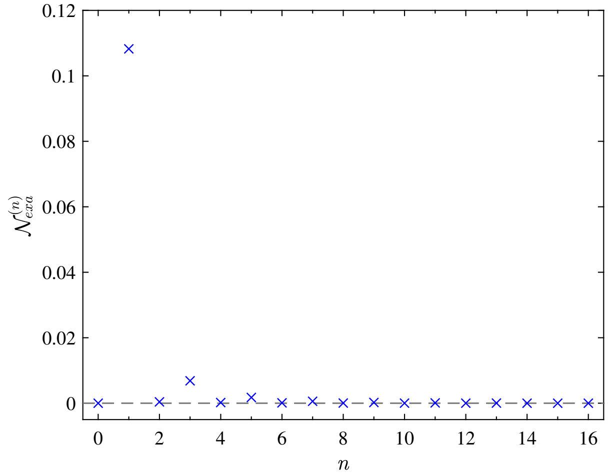

FIG. 6. The number of created particles $\mathcal{N}_{exa}^{(n)}$ (vertical axis) versus $n = \omega L_0/\pi$ (horizontal axis), for the law of motion given in Eq. (16), with $T = 2L_0$, $a = \varepsilon L_0$, $L_0 = l_0 = 1$ and $\varepsilon = 10^{-1}$ (maximum velocity $v \approx 0.6$). The dashed line serves as a reference for the value $\mathcal{N}_{exa}^{(n)} = 0$. Note that $n = 1$ represents half of the oscillation frequency, and $n = 2$ indicates the oscillation frequency ω_0. For $n = 3$ and $n = 5$, one can see the creation of particles with frequencies larger than $\omega_0 = 2\pi$ $(n = 2)$.

Fig. 6 one can see the creation of particles with frequencies $3\pi/L_0$ (mode $n = 3$) and $5\pi/L_0$ $(n = 5)$. Since this particle creation with frequencies above ω_0 is not related to the reinteractions of perturbed field modes with the right mirror in a state of motion, but caused only by the relativistic aspect (in this case, $v \approx 0.6$) of the mirror's motion, this region of frequencies with $(\omega > \omega_0)$ is called a relativistic band [29].

To estimate the relevance of the relativistic band as the maximum velocity of oscillation increases, we consider

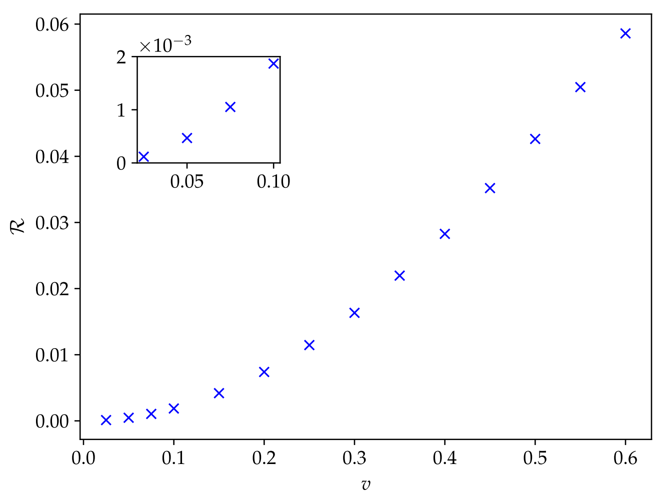

FIG. 7. The ratio $\mathcal{R} = \mathcal{N}_{exa}^{(3)}/\mathcal{N}_{exa}^{(1)}$ (vertical axis) versus $v = 2\pi a$ (horizontal axis), where a is the amplitude of oscillation given in the law of motion in Eq. (16), with $T = 2L_0$, $L_0 = l_0 = 1$.

Eq. (16) with $L_0 = l_0 = 1$, and a $(v = 2\pi a)$ varying from 0 $(v = 0)$ to 0.1 $(v \approx 0.6)$. In Fig. 7, we show [using Eq. (14)] the behavior of the ratio $\mathcal{R} = \mathcal{N}_{exa}^{(3)}/\mathcal{N}_{exa}^{(1)}$ as a function of v. We highlight the following results: $v \approx 2\pi \times 10^{-3} \Rightarrow \mathcal{R} \approx 7.4 \times 10^{-6}$; $v \approx 2\pi \times 10^{-2} \Rightarrow \mathcal{R} \approx 7.4 \times 10^{-4}$ (these values correspond to the case shown in Fig. 5, and the low value of $\mathcal{R}$ explains the null visualization of a relativistic band); $v \approx 10^{-1} \Rightarrow \mathcal{R} \approx 1.9 \times 10^{-3}$ (this velocity is the maximum effective velocity considered by Wilson *et al.* in the first observation of the DCE [24]); $v \approx 3.0 \times 10^{-1} \Rightarrow \mathcal{R} \approx 1.6 \times 10^{-2}$ (this velocity is the maximum effective velocity considered in the experiment by Schneider *et al.* [28]); $v \approx 2\pi \times 10^{-1} \Rightarrow \mathcal{R} \approx 6.3 \times 10^{-2}$ (these values correspond to the relativistic band visualized in Fig. 6).

The increase of $\mathcal{R}$ with v, shown in Fig. 7, describes the formation of relativistic bands or, in other words, significant particle creation with frequencies above ω_0 caused only by the relativistic aspect of the mirror's motion.

V. CONNECTING DISCRETE AND CONTINUOUS RELATIVISTIC BANDS

In the present section, we investigate the connection between the relativistic band in the discrete spectrum shown in Fig. 6 and the relativistic band in a continuous spectrum for a relativistic oscillating single mirror [31].

Let us start the investigation by examining the spectrum shown in Fig. 5, where one can see that the creation of particles occurs only for the frequency $\omega_0/2$ and, consequently, there is no creation of particles with frequency beyond ω_0. Although Fig. 5 does not look like a parabola, the result shown in this figure is deeply connected to the parabolic continuous spectrum of a single moving mirror with nonrelativistic velocities [30], for which the spectral distribution has a maximum at $\omega_0/2$ and there is no particle creation with frequencies higher than ω_0. To clarify this connection, let us compare the cases of cavities with the moving mirror oscillating according to Eq. (16), with a fixed frequency $\omega_0 = 2\pi$ (in other words a fixed value $l_0 = 1$), fixed amplitude of oscillation a, but with different values of L_0, with $T = 2L_0$. We reinforce that, since we are considering the condition $T = 2L_0$, all field modes, after being perturbed by the oscillating right mirror and reflected by the left static mirror, do not find the right mirror in a state of motion again. We also remark that this is an important condition in order to make the transition from a discrete spectrum to a continuous one (produced by a single moving mirror and discussed in the literature [30]), since the field modes, after being perturbed by an oscillating single mirror, go to infinity and never interact with the moving mirror again.

For the law of motion in Eq. (16), with $a = 10^{-2}$, $l_0 = 1$ $(\omega_0 = 2\pi$ and $v \approx 0.06)$ and $T = 2L_0$, we have for $L_0 = 1$ and $L_0 = 4$ the results shown in Fig. 5 and Fig. 8, respectively. One can see that, increasing L_0 [for instance

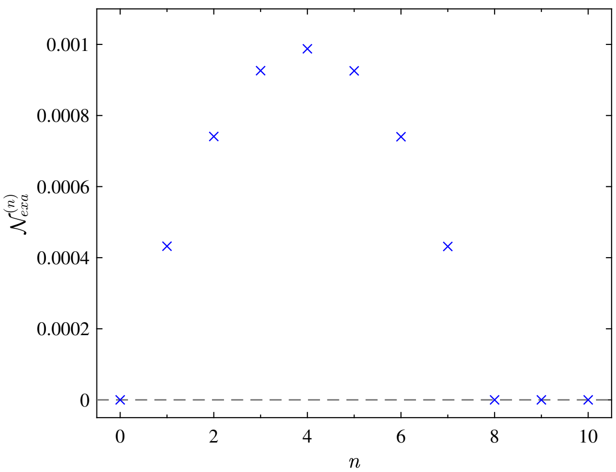

FIG. 8. The number of created particles $\mathcal{N}_{exa}^{(n)}$ (vertical axis) versus $n = \omega L_0/\pi$ (horizontal axis), for the law of motion given in Eq. (16), with $T = 2L_0$, $L_0 = 4$, $l_0 = 1$ and $a = 10^{-2}$ (maximum velocity $v = 2\pi a \approx 0.06$). The dashed line serves as a reference for the value $\mathcal{N}_{exa}^{(n)} = 0$. Note that $n = 4$ represents half of the oscillation frequency, and $n = 8$ indicates the oscillation frequency 2π. One can see that there is no creation of particles with frequency larger than 2π ($n = 8$).

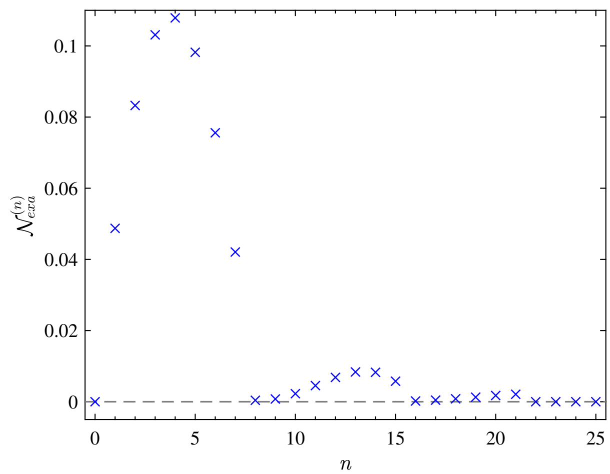

FIG. 9. The number of created particles $\mathcal{N}_{exa}^{(n)}$ (vertical axis) versus $n = \omega L_0/\pi$ (horizontal axis), for the law of motion given in Eq. (16), with $T = 2L_0$, $L_0 = 4$, $l_0 = 1$ and $a = 10^{-1}$ (maximum velocity $v = 2\pi a \approx 0.6$). The dashed line serves as a reference for the value $\mathcal{N}_{exa}^{(n)} = 0$. Note that $n = 4$ represents half of the oscillation frequency, and $n = 8$ represents the oscillation frequency 2π. One can see the creation of particles with frequencies larger than $\omega_0 = 2\pi$ ($n = 8$).

from $L_0 = 1$ (Fig. 5) to $L_0 = 4$ (Fig. 8)] and maintaining the same oscillation frequency 2π, particles are created with the frequency $\omega_0/2 = \pi$ and also with other frequencies smaller than ω_0. The discrete values obtained outline a parabolic spectrum (Fig. 8), with the maximum number of created particles with frequency π and no particles created with frequency higher than $\omega_0 = 2\pi$. This is in accordance with the predictions found in the literature for a continuous spectrum for a single oscillating mirror [30]. In other words, the spectrum shown in Fig. 5 is a germinal version of a spectrum with a parabolic shape, in the sense that, as L_0 is increased (but keeping the same frequency value), more and more the discrete spectrum outlines a continuous parabolic one. This reveals a consistency between the results obtained here [for the discrete spectra in a cavity provided by the exact formula (14)] and those found in the literature [30], for a continuous spectra for a nonrelativistic oscillating single mirror.

Now, we continue our investigation examining the spectrum shown in Fig. 6 (maximum velocity $v \approx 0.6$), which shows the creation of particles with frequency $\omega_0/2$, and also with frequencies above the oscillating frequency ω_0 (for instance $3\omega_0/2$ and $5\omega_0/2$). It also shows that the particle creation vanishes for all frequencies ω equal to an integer multiple of ω_0. Although one can say that Fig. 6 does not look like a succession of arches, the result shown in that figure is connected to the continuous spectrum for a relativistic oscillating single mirror, formed by a succession of arches, each one limited by two successive multiples of ω_0, and vanishing for all frequencies ω equal to an integer multiple of ω_0 [31]. To clarify this connection, let us consider the law motion in Eq. (16), with $a = 10^{-1}$, $l_0 = 1$ ($\omega_0 = 2\pi$ and $v \approx 0.6$), and $T = 2L_0$. We show in Fig. 6 and Fig. 9 the results for $L_0 = 1$ and $L_0 = 4$, respectively. Increasing L_0, for instance from $L_0 = 1$ (Fig. 6) to $L_0 = 4$ (Fig. 9), we see a population of particles created in several other frequency modes in addition to π, outlining a continuous spectrum formed by a succession of arches (Fig. 9), each one limited by two successive multiples of ω_0, and vanishing for all frequencies ω equal to an integer multiple of ω_0, in connection with the predictions found in the literature for a continuous spectrum for a single relativistic oscillating mirror [31]. The spectrum shown in Fig. 6 is then an initial version of a spectrum with a succession of arches, in the sense that, as L_0 is increased, more and more the discrete spectrum outlines a continuous succession of arches, exhibiting additional (relativistic) bands with frequencies higher then ω_0 [31]. Again, this reveals a consistency between the results for discrete spectra (cavity) provided by the exact formula (14) and those for continuous spectra for a relativistic oscillating single mirror found in the literature [31].

VI. FINAL REMARKS

In the present paper, we investigated the formation, via the dynamical Casimir effect, of relativistic bands in the discrete spectrum of created particles in an oscillating one-dimensional resonant cavity. We considered a real scalar field obeying Eq. (1), under the boundary conditions given in Eq. (2). We wrote, based on previous works in the literature [33–35], exact formulas for the spectrum [Eq. (14)] and total number of created particles [Eq. (15)]. Although these formulas are valid for an arbitrary prescribed law of motion for the oscillating mirror, we focused on the class of laws of motion given by Eq. (16), and, more specifically, considered $a = \varepsilon L_0$, $l_0 = L_0$ and $T = 2L_0/c$.

With the first two choices ($a = \varepsilon L_0$ and $l_0 = L_0$), Eq. (16) describes a resonant law of motion typically investigated in the context of the DCE [10,32], where the oscillation frequency is $\omega_0 = 2\pi/L_0$ (twice the frequency of the first mode π/L_0). In addition, the choice of the time of oscillation $T = 2L_0/c$ is such that a field mode, after being perturbed by the moving mirror, never meets this mirror in motion again (see Fig. 4). This allowed us to exclude the effect of the reinteraction of a perturbed field mode with the mirror in a state of motion, so that we could isolate only the role of the maximum speed of the mirror in creating particles with frequency above ω_0.

Using Eq. (14), we computed the spectrum of created particles when $v \approx 0.06c$ (Fig. 5) and $v \approx 0.6c$ (Fig. 6). In Fig. 5, we got no visible creation of particles with frequency above $\omega_0 = 2\pi/L_0$ (or no visualization of a relativistic band), with the creation of particles restricted to the first mode $n = 1$. More precisely, the relativistic band exists, but the number of particles is, for the mode $n = 3$, only approximately 7.4×10^{-4} of the number of created particles in the first mode. In Fig. 6, we can visualize an effective creation of particles with frequency above $\omega_0 = 2\pi/L_0$. In this case, the relativistic band is such that the number of particles for the mode $n = 3$ is approximately 6.3×10^{-2} of the number of created particles in the first mode. In Fig. 7, corresponding to Eq. (16) with $L_0 = l_0 = 1$, we describe the enhancement of the relativistic band in a discrete spectrum of created particles as the maximum velocity of oscillation increases.

Finally, we showed the connection between the relativistic band in the discrete spectrum shown in Fig. 6 and a relativistic band in a continuous spectrum (outlined in Fig. 9) for a relativistic oscillating single mirror [31]. Since relativistic bands for a continuous spectrum can, in principle, be observed [29], their detection will indicate the existence of relativistic bands in a discrete spectrum of created particles, as predicted here.

ACKNOWLEDGMENTS

The authors thank Alessandra N. Braga, Amanda E. da Silva, Andreson L. C. Rego, Edson C. M. Nogueira, Jeferson D. Lima Silva and Van Sérgio Alves for careful reading of this paper, fruitful discussions and suggestions. D. T. A. thanks the hospitality of the Centro de Física, Universidade do Minho, Braga, Portugal. E. R. G. thanks the hospitality of the Programa de Pós-Graduação em Física, Universidade Federal do Pará, Belém, Pará, Brazil.

[1] G. T. Moore, Quantum theory of the electromagnetic field in a variable-length one-dimensional cavity, J. Math. Phys. (N.Y.) **11**, 2679 (1970).
[2] B. S. DeWitt, Quantum field theory in curved spacetime, Phys. Rep. **19**, 295 (1975).
[3] S. A. Fulling and P. C. W. Davies, Radiation from a moving mirror in two dimensional space-time: conformal anomaly, Proc. R. Soc. A. **348**, 393 (1976).
[4] P. C. W. Davies and S. A. Fulling, Radiation from moving mirrors and from black holes, Proc. R. Soc. A **356**, 237 (1977).
[5] P. Candelas and D. Deutsch, On the vacuum stress induced by uniform acceleration or supporting the ether, Proc. R. Soc. A **354**, 79 (1977).
[6] V. V. Dodonov, Dynamical Casimir effect: Some theoretical aspects, J. Phys. Conf. Ser. **161**, 012027 (2009).
[7] V. V. Dodonov, Current status of the dynamical Casimir effect, Phys. Scr. **82**, 038105 (2010).
[8] D. A. R. Dalvit, P. A. M. Neto, and F. D. Mazzitelli, *Fluctuations, Dissipation and the Dynamical Casimir Effect*, edited by D. A. R. Dalvit, P. Milonni, D. Roberts, and F. da Rosa (Springer-Verlag, Berlin, Heidelberg, 2011), Chap. 13, pp. 419–457.
[9] V. Dodonov, Fifty years of the dynamical Casimir effect, Physics **2**, 67 (2020).
[10] V. V. Dodonov and A. B. Klimov, Generation and detection of photons in a cavity with a resonantly oscillating boundary, Phys. Rev. A **53**, 2664 (1996).
[11] W.-J. Kim, J. H. Brownell, and R. Onofrio, Detectability of Dissipative Motion in Quantum Vacuum via Superradiance, Phys. Rev. Lett. **96**, 200402 (2006).
[12] J. H. Brownell, W. J. Kim, and R. Onofrio, Modelling superradiant amplification of Casimir photons in very low dissipation cavities, J. Phys. A **41**, 164026 (2008).
[13] A. Motazedifard, A. Dalafi, M. Naderi, and R. Roknizadeh, Controllable generation of photons and phonons in a coupled Bose-Einstein condensate-optomechanical cavity via the parametric dynamical Casimir effect, Ann. Phys. (Amsterdam) (N.Y). **396**, 202 (2018).
[14] M. Sanz, W. Wieczorek, S. Gröblacher, and E. Solano, Electro-mechanical Casimir effect, Quantum **2**, 91 (2018).
[15] W. Qin, V. Macrì, A. Miranowicz, S. Savasta, and F. Nori, Emission of photon pairs by mechanical stimulation of the squeezed vacuum, Phys. Rev. A **100**, 062501 (2019).

[16] S. Butera and I. Carusotto, Mechanical backreaction effect of the dynamical Casimir emission, Phys. Rev. A **99**, 053815 (2019).

[17] E. Yablonovitch, Accelerating Reference Frame for Electromagnetic Waves in a Rapidly Growing Plasma: Unruh-Davies-Fulling-Dewitt Radiation and the Nonadiabatic Casimir Effect, Phys. Rev. Lett. **62**, 1742 (1989).

[18] Y. E. Lozovik, V. G. Tsvetus, and E. A. Vinogradov, Femtosecond parametric excitation of electromagnetic field in a cavity, JETP Lett. **61**, 723 (1995).

[19] C. Braggio, G. Bressi, G. Carugno, C. Del Noce, G. Galeazzi, A. Lombardi, A. Palmieri, G. Ruoso, and D. Zanello, A novel experimental approach for the detection of the dynamical Casimir effect, Europhys. Lett. **70**, 754 (2005).

[20] A. Agnesi, C. Braggio, G. Bressi, G. Carugno, G. Galeazzi, F. Pirzio, G. Reali, G. Ruoso, and D. Zanello, MIR status report: An experiment for the measurement of the dynamical Casimir effect, J. Phys. A **41**, 164024 (2008).

[21] A. Agnesi, C. Braggio, G. Bressi, G. Carugno, F. D. Valle, G. Galeazzi, G. Messineo, F. Pirzio, G. Reali, G. Ruoso, D. Scarpa, and D. Zanello, MIR: An experiment for the measurement of the dynamical Casimir effect, J. Phys. Conf. Ser. **161**, 012028 (2009).

[22] J. R. Johansson, G. Johansson, C. M. Wilson, and F. Nori, Dynamical Casimir Effect in a Superconducting Coplanar Waveguide, Phys. Rev. Lett. **103**, 147003 (2009).

[23] F. X. Dezael and A. Lambrecht, Analogue Casimir radiation using an optical parametric oscillator, Europhys. Lett. **89**, 14001 (2010).

[24] C. M. Wilson, G. Johansson, A. Pourkabirian, M. Simoen, J. R. Johansson, T. Duty, F. Nori, and P. Delsing, Observation of the dynamical Casimir effect in a superconducting circuit, Nature (London) **479**, 376 (2011).

[25] P. Lähteenmäki, G. S. Paraoanu, J. Hassel, and P. J. Hakonen, Dynamical Casimir effect in a Josephson metamaterial, Proc. Natl. Acad. Sci. U.S.A. **110**, 4234 (2013).

[26] A. Motazedifard, M. H. Naderi, and R. Roknizadeh, Analogue model for controllable Casimir radiation in a nonlinear cavity with amplitude-modulated pumping: Generation and quantum statistical properties, J. Opt. Soc. Am. B **32**, 1555 (2015).

[27] S. Vezzoli, A. Mussot, N. Westerberg, A. Kudlinski, H. D, Saleh, A. Prain, F. Biancalana, E. Lantz, and D. Faccio, Optical analogue of the dynamical Casimir effect in a dispersion-oscillating fibre, Commun. Phys. **2**, 84 (2019).

[28] B. H. Schneider, A. Bengtsson, I. M. Svensson, T. Aref, G. Johansson, J. Bylander, and P. Delsing, Observation of Broadband Entanglement in Microwave Radiation from a Single Time-Varying Boundary Condition, Phys. Rev. Lett. **124**, 140503 (2020).

[29] A. L. C. Rego, J. P. d. S. Alves, D. T. Alves, and C. Farina, Relativistic bands in the spectrum of created particles via the dynamical Casimir effect, Phys. Rev. A **88**, 032515 (2013).

[30] A. Lambrecht, M.-T. Jaekel, and S. Reynaud, Motion Induced Radiation from a Vibrating Cavity, Phys. Rev. Lett. **77**, 615 (1996).

[31] A. Lambrecht, M. T. Jaekel, and S. Reynaud, Frequency up-converted radiation from a cavity moving in vacuum, Eur. Phys. J. D **3**, 95 (1998).

[32] V. V. Dodonov, A. B. Klimov, and D. E. Nikonov, Quantum phenomena in resonators with moving walls, J. Math. Phys. (N.Y.) **34**, 2742 (1993).

[33] V. V. Dodonov, A. B. Klimov, and V. I. Man'ko, Generation of squeezed states in a resonator with a moving wall, Phys. Lett. A **149**, 225 (1990).

[34] P. Węgrzyn, Quantum energy in a vibrating cavity, Mod. Phys. Lett. A **19**, 769 (2004).

[35] C. K. Cole and W. C. Schieve, Radiation modes of a cavity with a moving boundary, Phys. Rev. A **52**, 4405 (1995).

[36] D. T. Alves, E. R. Granhen, H. O. Silva, and M. G. Lima, Quantum radiation force on the moving mirror of a cavity, with Dirichlet and Neumann boundary conditions for a vacuum, finite temperature, and a coherent state, Phys. Rev. D **81**, 025016 (2010).

[37] D. T. Alves and E. R. Granhen, A computer algebra package for calculation of the energy density produced via the dynamical Casimir effect in one-dimensional cavities, Comput. Phys. Commun. **185**, 2101 (2014).

[38] M. Razavy and J. Terning, Quantum radiation in a one-dimensional cavity with moving boundaries, Phys. Rev. D **31**, 307 (1985).

[39] M. Castagnino and R. Ferraro, The radiation from moving mirrors: The creation and absorption of particles, Ann. Phys. (N.Y.) **154**, 1 (1984).

[40] M. Ruser, Vibrating cavities: A numerical approach, J. Opt. B **7**, S100 (2005).

[41] N. D. Antunes, Numerical simulation of vacuum particle production: Applications to cosmology, dynamical Casimir effect and time dependent nonhomogeneous dielectrics, arXiv:hep-ph/0310131.

[42] M. Ruser, Numerical approach to the dynamical Casimir effect, J. Phys. A **39**, 6711 (2006).

[43] F. C. Lombardo, F. D. Mazzitelli, A. Soba, and P. I. Villar, Dynamical Casimir effect in superconducting circuits: A numerical approach, Phys. Rev. A **93**, 032501 (2016).

[44] P. I. Villar, A. Soba, and F. C. Lombardo, Numerical approach to simulating interference phenomena in a cavity with two oscillating mirrors, Phys. Rev. A **95**, 032115 (2017).

[45] P. I. Villar and A. Soba, Adaptive numerical algorithms to simulate the dynamical Casimir effect in a closed cavity with different boundary conditions, Phys. Rev. E **96**, 013307 (2017).

[46] D. T. Alves, C. Farina, and E. R. Granhen, Dynamical Casimir effect in a resonant cavity with mixed boundary conditions, Phys. Rev. A **73**, 063818 (2006).